IEEE Access
Multidisciplinary ⋮ Rapid Review ⋮ Open Access Journal

Received 24 July 2024, accepted 1 September 2024, date of publication 5 September 2024, date of current version 17 September 2024.

Digital Object Identifier 10.1109/ACCESS.2024.3454820

RESEARCH ARTICLE

A Novel Four-Dimensional Hyperchaotic System: Design, Dynamic Analysis, Synchronization, and Image Encryption

ERMAN OZPOLAT[1], VEDAT CELIK[2], AND ARIF GULTEN[2]

[1]Department of Electrical and Electronics Engineering, Faculty of Engineering and Architecture, Muş Alparslan University, 49100 Muş, Türkiye
[2]Department of Electrical and Electronics Engineering, Faculty of Engineering, Firat University, 23119 Elâzığ, Türkiye

Corresponding author: Erman Ozpolat (e.ozpolat@alparslan.edu.tr)

This work was supported by Firat University Research Fund under Project MF.24.51.

ABSTRACT This study comprehensively examines the design, dynamic analysis, and various application areas of a novel four-dimensional hyperchaotic system, which has not been previously utilized in the literature. The dynamic properties of the proposed hyperchaotic system are analyzed in detail, including bifurcation diagrams, Lyapunov exponents, phase diagrams, and sensitivity to initial conditions. The system behaves in a hyperchaotic manner, as verified by the dynamic analysis. Additionally, the physical feasibility of the system is tested through circuit simulations performed on the Multisim 14.3 platform. Within the scope of the study, synchronization of the proposed hyperchaotic system is achieved using active control methods, and the system is successfully applied in image encryption and decryption application. In this context, the advantages of hyperchaotic systems in terms of encryption security are emphasized. The obtained results demonstrate that the proposed four-dimensional hyperchaotic system can be effectively used in image encryption applications, offering significant potential in this field. This study can be considered an important step towards enhancing the role and effectiveness of hyperchaotic systems in secure communication implementations.

INDEX TERMS Chaos, hyperchaotic system, active control synchronization, image encryption.

I. INTRODUCTION

The Lorenz system, discovered by Lorenz during his studies on atmospheric convection and named after him, represents a significant milestone as the first three-dimensional chaotic system [1], [2]. Following the Lorenz system, many chaotic systems have been proposed by scientists. The most notable among them are the Chua chaotic circuit and the Chen chaotic system [3], [4]. Subsequently, the Lü system was discovered, and Lü and his colleagues proposed a unified chaotic system capable of representing three different chaotic systems as special cases [5], [6].

After the first four-dimensional hyperchaotic system was introduced by Rössler, the concept of hyperchaos began to attract more interest from scientists [7]. The most significant difference between hyperchaotic and chaotic systems is that hyperchaotic systems possess two positive Lyapunov exponents. Also, hyperchaotic systems have a more complex structure compared to chaotic systems. In recent years, numerous studies on hyperchaotic systems have appeared in the literatures [8], [9], [10], and [11]. Hyperchaotic systems have many application areas, with one of the most significant being synchronization applications. Since chaotic and hyperchaotic systems are extremely sensitive to initial conditions, even the smallest differences in initial conditions lead to substantial variations between the systems. Chaos synchronization was first achieved by Pecora and Carroll [12]. The chaos synchronization proposed by Pecora and Carroll was later developed by scientists, leading to the proposal of many different synchronization methods [13], [14], [15], [16], [17]. Therefore, chaos synchronization, or in other words, chaos control, has gained considerable importance [18].

The associate editor coordinating the review of this manuscript and approving it for publication was Jun Wang.

Synchronization applications are typically used in secure communication and image encryption fields.

In image encryption applications, chaotic systems are used to securely encrypt and decrypt image data [19], [20], [21], [22], [23]. A chaotic signal is used to encrypt the image data, and only a synchronized chaotic system can accurately decrypt this data. This method is particularly effective in protecting sensitive or confidential images.

Emiroglu et al. [24] proposed a new four-dimensional hyperchaotic system using the T chaotic system in their study. After conducting the dynamic analysis and circuit implementation of the proposed hyperchaotic system, they successfully achieved synchronization of the proposed system using a passive control method. Nestor et al. [25] introduced a new 4D hyperchaotic nonlinear dynamic system with two positive Lyapunov exponents in their work. They performed dynamic analysis of the proposed hyperchaotic system, which contains hidden attractors. Subsequently, they implemented the circuit and applied an adaptive synchronization method. Li et al. [26] performed module synchronization between a hyperchaotic real system and its corresponding complex system in their study. They designed the systems and examined their dynamic analyses. An adaptive controller was designed based on the Lyapunov stability theory, and successful results were obtained from simulations. Yan et al. [27] designed an image encryption algorithm using finite-time synchronization based on a multi-scroll hyperchaotic system. They employed a novel cutting and shuffling method in the algorithm, achieving successful results in image encryption. He et al. [28] utilized master-slave synchronization for hyperchaotic systems in their study. To reduce disturbances in master-slave synchronization, they intermittently activated the controller, enhancing security. This structure was used in image encryption algorithms, yielding successful results.

In recent years, research on image encryption has gained significant importance. Particularly, the use of chaotic systems in image encryption applications provides substantial advantages in terms of encryption security. A review of recent studies shows that chaotic systems are generally preferred. However, encryption applications using hyperchaotic systems, due to their more complex structure compared to chaotic systems, further enhance the reliability of encryption. A review of the literature reveals that the synchronization of hyperchaotic systems in image encryption applications is less frequently utilized, which served as a motivation for this study.

The study's original and innovative contributions to the literature can be summed up as follows:

- It proposes a four-dimensional hyperchaotic system that has never been used in the literature before. We have performed dynamic assessments of this new type of hyperchaotic system.
- A circuit simulation was run on the Multisim 14.3 platform to evaluate the proposed four-dimensional hyperchaotic system's physical viability.
- Active control was used to achieve the synchronization design of the proposed hyperchaotic system.
- Image encryption was performed using this novel hyperchaotic system, and decryption was achieved through synchronization design.

This paper proposes a new four-dimensional hyperchaotic system that has never been used in the literature before. After the relevant dynamic assessments of the proposed hyperchaotic system were completed, the Multisim 14.3 platform was used to create a circuit simulation. The active control mechanism was used to synchronize the suggested four-dimensional hyperchaotic system. This synchronization structure was then successfully evaluated in image encryption and decryption implementations. Figure 1 shows a schematic of the suggested study.

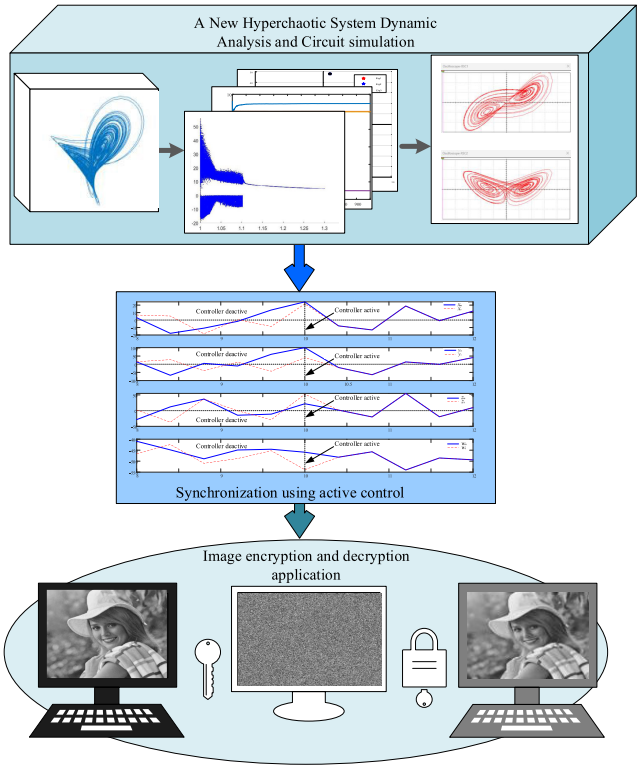

FIGURE 1. A schematic of the study.

The remaining sections of the research are arranged as follows: The mathematical model of the suggested four-dimensional hyperchaotic system is offered in Section II, along with a description of the innovative 4-dimensional hyperchaotic system and its dynamical analysis presented in this paper. Section III develops the proposed hyperchaotic system's circuit model and conducts simulations. Section IV presents simulation findings and describes in detail how the proposed revolutionary four-dimensional hyperchaotic system is synchronized utilizing active control. In Section V, image encryption and decryption applications are carried out using the synchronization structure of the proposed novel four-dimensional hyperchaotic system. Finally, Section VI presents the conclusions of the study.

II. A NOVEL 4-DIMENSIONAL HYPERCHAOTIC SYSTEM AND DYNAMIC ANALYSES

In this section of the paper, the mathematical formulations of the proposed novel 4-dimensional hyperchaotic system will be presented and the dynamical analysis of the proposed hyperchaotic system will be carried out.

A. PROPOSED HYPERCHAOTIC SYSTEM

The mathematical expressions for the proposed novel hyperchaotic system, which consists of 11 terms with three second-order nonlinear states, are shown in (1).

$$\begin{aligned} \dot{x} &= -24x + 8y \\ \dot{y} &= ax + y - 2xz \\ \dot{z} &= bxy - 4z + w \\ \dot{w} &= -xy - 2z - w \end{aligned} \tag{1}$$

In the system, a and b are positive parameters, while x, y, z, and w represent the states of the hyperchaotic system. The system exhibits hyperchaotic behavior under certain positive parameter values of a and b and specific initial conditions. It is notable for its ability to display significantly different behavior with varying initial values.

B. DYNAMIC ANALYSES

In this section, various analyses will be conducted to examine whether the proposed hyperchaotic system exhibits hyperchaotic behavior. There are several dynamic analysis methods available to observe chaotic or hyperchaotic behavior in systems.

Firstly, the bifurcation diagram analysis of the hyperchaotic system will be investigated. The bifurcation diagram is an analytical method used to determine parameter values for chaotic systems. Figure 2 shows the bifurcation diagram for the proposed system. When plotting the bifurcation diagram, the parameter a was set to 20, and the value of the parameter b was varied between 1 and 1.3. The system's initial values were taken as [1 1 1 1].

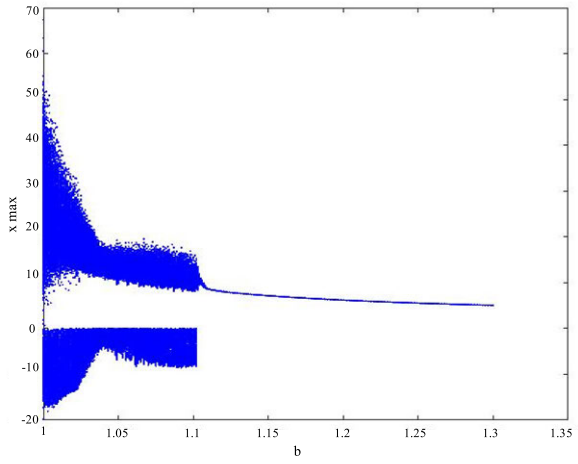

FIGURE 2. Bifurcation diagram for b parameter.

It can be seen from the bifurcation diagram that the system behaves chaotically when the parameter b is between 1 and 1.1. Therefore, for the proposed system, the parameter a was selected as 20, and the parameter b was chosen as 40/39. These values will be used for the remainder of the study.

One of the most important characteristics for investigating hyperchaotic behavior in systems is the analysis of Lyapunov exponents. Hyperchaotic systems possess at least two positive Lyapunov exponents. In this study, the Lyapunov exponents were calculated using the Allen Wolf algorithm [29]. The variation of the Lyapunov exponents for the proposed hyperchaotic system is shown in Figure 3. The initial conditions for the system were set as [1 1 1 1] when calculating the Lyapunov exponents.

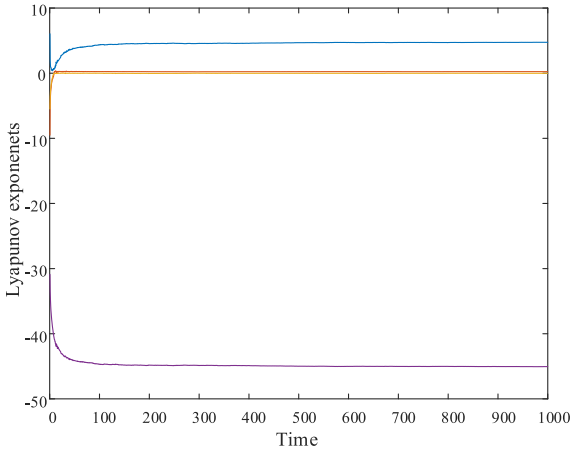

FIGURE 3. Variation of the Lyapunov exponents with respect to time.

The Lyapunov exponents of the proposed system were calculated as $L_1 = 4.742, L_2 = 0.061, L_3 = 0$ and $L_4 = -45.046$. The system exhibits hyperchaotic behavior due to having two positive Lyapunov exponents.

Under these parameter values, the phase space diagrams and time series of the proposed hyperchaotic system clearly indicate chaotic behavior. The phase space diagrams and the three-dimensional phase portrait of the proposed hyperchaotic system are shown in Figure 4. The initial conditions for the system during simulation were set as [1 1 1 1].

Examining the phase space diagrams of the system clearly reveals that the system has strange attractors and dynamic oscillations. Therefore, it can be said that the system exhibits hyperchaotic behavior.

Furthermore, Figure 5 shows the time series of the state variable x and the change of the error when [1 1 1 1] and [1.01 1 1 1] are selected so that the initial conditions are very close.

As seen from Figure 5, while the values of the y state variable are the same during the first 10 seconds, they diverge after the 10th second. This behavior indicates that the proposed system exhibits sensitivity to initial conditions, which is a key characteristic of hyperchaotic systems.

One of the dynamic analysis methods for hyperchaotic systems is the Kaplan-Yorke dimension [30]. Hyperchaotic

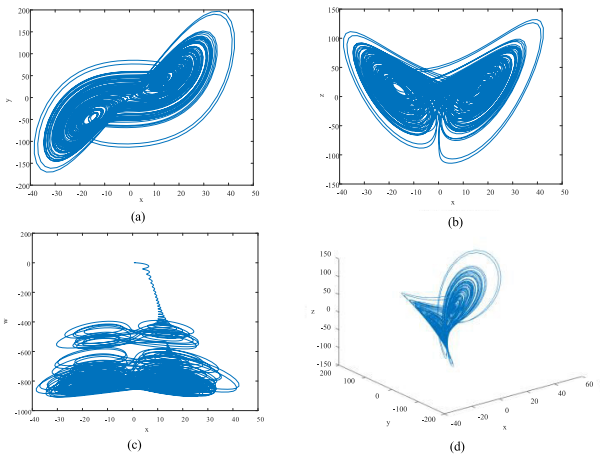

FIGURE 4. (a) x - y phase diagram, (b) x - z phase diagram, (c) x - w phase diagram, (d) x - y - z three-dimensional phase portrait.

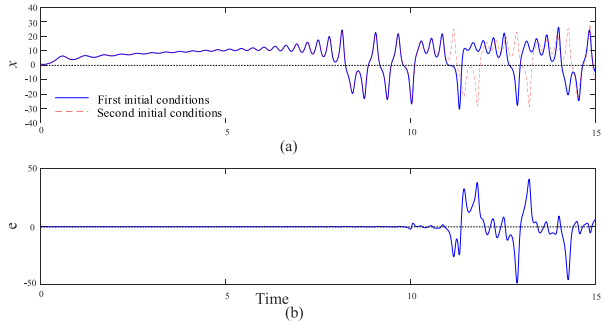

FIGURE 5. (a) Time series of the x state variable for closely spaced initial conditions, (b) Error variation of the x state variable for closely spaced initial conditions.

systems inevitably exhibit fractal behavior. The degree of predictability of the system can be derived from the fractal dimension of the attractor A deterministic system most likely produced the data if the fractal dimension is small. A random system is most likely the source of the data if the fractal dimension is huge. Because its structure is unlike any other geometric creation, fractal dimensions are the explanation offered by researchers for it [31]. The Kaplan-Yorke dimension of the proposed hyperchaotic system was calculated as shown in (2).

$$D_L = j + \frac{1}{|L_j + 1|}\sum_{i=1}^{j} L_i = 3 + \frac{L_1 + L_2 + L_3}{|L_4|} = 3.106 \tag{2}$$

As observed, the Lyapunov dimension of the proposed system is fractional. The proposed system exhibits non-periodic orbits and varying nearby paths due to its fractal nature. Hence, the proposed nonlinear system demonstrates hyperchaotic behavior.

Another method is dissipation analysis [32]. The divergence of the proposed system is calculated in (3).

$$div\Phi = \frac{\partial \dot{x}}{\partial x} + \frac{\partial \dot{y}}{\partial y} + \frac{\partial \dot{z}}{\partial z} + \frac{\partial \dot{w}}{\partial w} = -24 + 1 - 4 - 1 = -28 \tag{3}$$

Since the divergence of the system's vector field is negative, it indicates that the system is dissipative. Therefore, it can be concluded that the system may have strange attractors.

The proposed hyperchaotic system also possesses symmetry properties. Examination of (4) clearly shows that the system is symmetric around the z and w axes.

$$(x, y, z, w) \rightarrow (-x, -y, z, w) \tag{4}$$

This indicates that the system is invariant.

Another important analysis for the dynamic analysis of hyperchaotic systems is the analysis of equilibrium points. The suggested system's equilibrium points can only be found when all of its state equations are set to zero. Using (5), the equilibrium points of the suggested hyperchaotic system were found.

$$\begin{aligned} 0 &= -24x + 8y \\ 0 &= ax + y - 2xz \\ 0 &= bxy - 4z + w = 0 \\ 0 &= -xy - 2z - w = 0 \end{aligned} \tag{5}$$

When the necessary calculations are performed with $a = 20$ and $b = 40/39$, three equilibrium points of the proposed hyperchaotic system are found. These are $E_1 = [0\ 0\ 0\ 0]$, $E_2 = [29.9489.8411.5 - 2714]$ and $E_3 = [-29.94 - 89.8411.5 - 2714]$. To analyze the stability of the proposed hyperchaotic system, the eigenvalues of the system must be determined. To find the eigenvalues, the Jacobian matrix of the proposed hyperchaotic system is first required. The Jacobian matrix of the system is shown in (6).

$$J = \begin{bmatrix} -24 & 8 & 0 & 0 \\ 20 - 2z & 1 & -2x & 0 \\ \frac{40y}{39} & \frac{40x}{39} & -4 & 1 \\ -y & -x & -2 & -1 \end{bmatrix} \tag{6}$$

The eigenvalues of the system for the equilibrium points E_1, E_2 and E_3 were determined using the formula $|J - \lambda I| = 0$. These eigenvalues are provided in Table 1.

Additionally, the calculated eigenvalues for the proposed hyperchaotic system are detailed in Figure 6. Upon examining the calculated eigenvalues, it is observed that some of them are in the unstable region, meaning they have positive eigenvalues. Therefore, the proposed hyperchaotic system has strange attractor.

III. ELECTRONIC CIRCUIT IMPLEMENTATION

The circuit simulation application of dynamic systems plays a crucial role in practical chaos-based applications [33], [34]. In this section of the study, the circuit implementation of the proposed 4-dimensional hyperchaotic system will be conducted. This design will be created to further validate the dynamic behavior of the chaotic system following the theoretical analyses and numerical simulations performed for the proposed 4-dimensional hyperchaotic system. The circuit implementation was designed using the Multisim 14.3 circuit

TABLE 1. Eigenvalues corresponding to the equilibrium points.

E_i	Equilibrium Points	Eigenvalues
E_1	[0 0 0 0]	[−3 −2 −29.28 6.28]
E_2	[29.94 89 11.5 −2714]	[4.95 ± j48.07 −0.02 −37.87]
E_3	[−29.94 −89 11.5 −2714]	[4.95 ± j48.07 −0.02 −37.87]

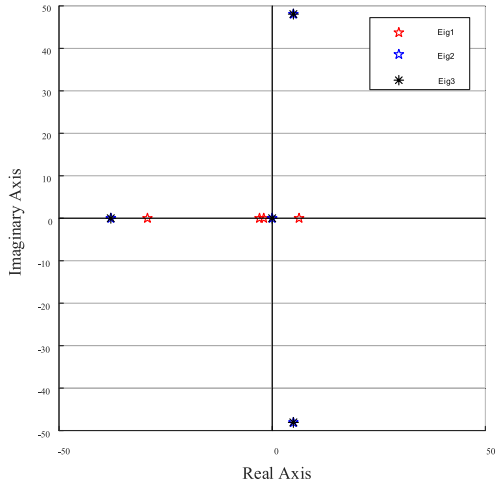

FIGURE 6. Representation of the eigenvalues in the *s*-plane.

simulation software. In the circuit design, Kirchhoff's laws were considered, and operational amplifiers (TL084ACN), multipliers (IC AD633), resistors, and capacitors were used. The power supply voltage for the operational amplifiers is ±15V. The electrical circuit equations for the proposed hyperchaotic system with parameters $a = 20$ and $b = 40/39$ are shown in (7).

$$\begin{aligned}
\dot{x} &= \frac{1}{C_1}\left[\frac{1}{R_1}x + \frac{1}{R_2}\left(\frac{R_9}{R_8}\right)(-y)\right] \\
\dot{y} &= \frac{1}{C_2}\left[\frac{1}{R_{10}}\left(\frac{R_4}{R_3}\right)(-x) + \frac{1}{R_6}\left(\frac{R_9}{R_8}\right)(-y) + \frac{1}{R_7}\frac{xz}{10}\right] \\
\dot{z} &= \frac{1}{C_3}\left[\frac{1}{R_{12}}\left(\frac{R_4}{R_3}\right)\frac{(-x)\,y}{10} + \frac{1}{R_{11}}z + \frac{1}{R_{17}}\left(\frac{R_{16}}{R_{15}}\right)(-w)\right] \\
\dot{w} &= \frac{1}{C_4}\left[\frac{1}{R_{13}}\frac{xy}{10} + \frac{1}{R_{20}}z + \frac{1}{R_5}w\right]
\end{aligned} \tag{7}$$

The values of the circuit components acquired after carrying out the required computations are given in Table 2.

Considering the calculated circuit components, the circuit model created on the Multisim 14.3 platform is shown in Figure 7.

As shown in Figure 7, the circuit consists of 7 operational amplifiers, 4 capacitors, 3 multipliers, 17 resistors, and 2 dual-channel oscilloscopes used for observing phase space diagrams. During the simulation, the initial conditions for the hyperchaotic system were set to [1 1 1 1]. The resulting oscilloscope images are provided in Figure 8.

Upon examining the obtained oscilloscope images, it was observed that Figure 8 (a), showing the x y phase space diagram, is similar to Figure 4 (a), and Figure 8 (b), showing

TABLE 2. Values of the circuit components used.

Circuit Elements	Labels	Values
Resistance	$R_3R_4R_8R_9R_{15}R_{16}$	100 $k\Omega$
	R_1	0.416 $k\Omega$
	R_2	1250 $k\Omega$
	$R_5R_6R_{17}$	10 $k\Omega$
	R_7R_{10}	0.5 $k\Omega$
	R_{11}	2.5 $k\Omega$
	R_{12}	0.975 $k\Omega$
	R_{13}	1 $k\Omega$
	R_{20}	5 $k\Omega$
Capacitance	$C_1C_2C_3C_4$	100 nF

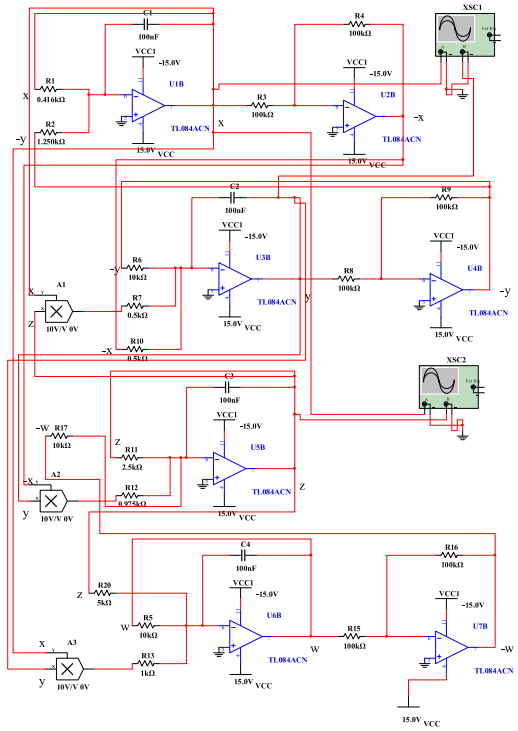

FIGURE 7. Circuit model of the proposed 4-dimensional hyperchaotic system.

the x z phase space diagram, is similar to Figure 4 (b). The results obtained from the circuit model of the proposed 4-dimensional hyperchaotic system, using the Multisim platform, provide strong validation for the presence of hyperchaotic attractors. Furthermore, the noted correspondences among the outcomes aid with the instantaneous execution of the suggested hyperchaotic framework.

IV. SYNCHRONIZATION OF THE NOVEL HYPERCHAOTIC SYSTEM USING ACTIVE CONTROL

In this section of the study, the synchronization of the proposed four-dimensional hyperchaotic system will be achieved using active control methods. Identical four-dimensional hyperchaotic systems have been used in the synchronization design. One of the identical hyperchaotic systems is designed as the receiver and the other as the transmitter [35]. A block

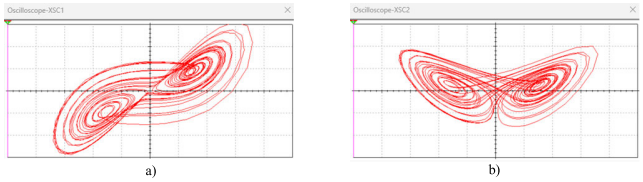

FIGURE 8. (a) Oscilloscope representation of x y phase space diagram, (b) Oscilloscope representation of x z phase space.

diagram of the created synchronization structure is shown in Figure 9.

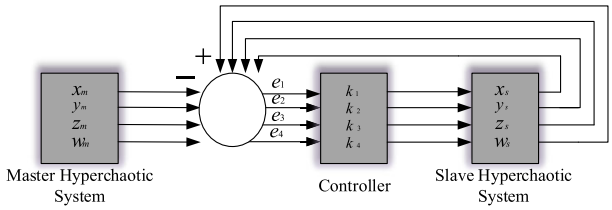

FIGURE 9. Block diagram of the synchronization structure.

To achieve this synchronization, it is necessary to obtain the error dynamics under different initial conditions. The master hyperchaotic system is provided in (8).

$$\begin{aligned}\dot{x}_m &= -24x_m + 8y_m \\ \dot{y}_m &= ax_m + y_m - 2x_m z_m \\ \dot{z}_m &= bx_m y_m - 4z_m + w_m \\ \dot{w}_m &= -x_m y_m - 2z_m - w_m \end{aligned} \tag{8}$$

In (9) illustrates the slave hyperchaotic system.

$$\begin{aligned}\dot{x}_s &= -24x_s + 8y_s + \mu_a(t) \\ \dot{y}_s &= ax_s + y_s - 2x_s z_s + \mu_b(t) \\ \dot{z}_s &= bx_s y_s - 4z_s + w_s + \mu_c(t) \\ \dot{w}_s &= -x_s y_s - 2z_s - w_s + \mu_d(t) \end{aligned} \tag{9}$$

In (9), four control functions, $\mu_a(t)$, $\mu_b(t)$, $\mu_c(t)$ and $\mu_d(t)$ have been added to the slave hyperchaotic system. To compute these control functions, (8) is subtracted from (9), while using the error dynamics, i.e. $e_1 = x_s - x_m$, $e_2 = y_s - y_m$, $e_3 = z_s - z_m$, and $e_4 = w_s - w_m$, to obtain (10).

$$\begin{aligned}\dot{e}_1 &= -24e_1 + 8e_2 + \mu_a(t) \\ \dot{e}_2 &= ae_1 + e_2 - 2x_s z_s + 2x_m z_m + \mu_b(t) \\ \dot{e}_3 &= b(x_s y_s - x_m y_m) - 4e_3 + e_4 + \mu_c(t) \\ \dot{e}_4 &= -x_s y_s + x_m y_m - 2e_3 - e_4 + \mu_d(t) \end{aligned} \tag{10}$$

To eliminate the nonlinear terms, the appropriate active control functions are chosen as given in (11).

$$\begin{aligned}\mu_a(t) &= V_a(t) \\ \mu_b(t) &= 2x_s z_s - 2x_m z_m + V_b(t) \\ \mu_c(t) &= b(-x_s y_s + x_m y_m) + V_c(t) \\ \mu_d(t) &= x_s y_s - x_m y_m + V_d(t) \end{aligned} \tag{11}$$

Subsequently, substituting the control functions into (10) yields the linear form of the error dynamics, as given in (12).

$$\begin{aligned}\dot{e}_1 &= -24e_1 + 8e_2 + V_a(t) \\ \dot{e}_2 &= ae_1 + e_2 + V_b(t) \\ \dot{e}_3 &= -4e_3 + e_4 + V_c(t) \\ \dot{e}_4 &= -2e_3 - e_4 + V_d(t) \end{aligned} \tag{12}$$

In this context, $V_a(t) = -k_1 e_1$, $V_b(t) = -k_2 e_2$, $V_c(t) = -k_3 e_3$ and $V_d(t) = -k_4 e_4$ are selected. The matrix form of the linearized error dynamics is shown in (13).

$$\begin{bmatrix}\dot{e}_1 \\ \dot{e}_2 \\ \dot{e}_3 \\ \dot{e}_4\end{bmatrix} = \begin{bmatrix}-(24+k_1) & 8 & 0 & 0 \\ a & 1-k_2 & 0 & 0 \\ 0 & 0 & 0\,(4+k_3) & 1 \\ 0 & 0 & -2 & -(1+k_4)\end{bmatrix}\begin{bmatrix}e_1 \\ e_2 \\ e_3 \\ e_4\end{bmatrix} \tag{13}$$

Using the coefficient matrix from the matrix provided in (13), the resulting characteristic equation is given in (14).

$$\begin{aligned}&\left(k_3 + 4k_4 + 5\lambda + k_3k_4 + k_3\lambda + k_4\lambda + \lambda^2 + 6\right) \\ &\times\left(24k_2 - k_1 - 8a + 23\lambda + k_1k_2 + k_1\lambda + k_2\lambda + \lambda^2 - 24\right) = 0\end{aligned} \tag{14}$$

In the proposed hyperchaotic system, the parameter a was chosen to be 20. When all k values were selected as 20, the eigenvalues of the error dynamics were calculated as $\lambda_1 = -23$, $\lambda_2 = -22$, $\lambda_3 = -49.28$ and $\lambda_4 = -13.71$. This result indicates that the error dynamics are stable for the chosen k values aimed at synchronization.

A. NUMERICAL SIMULATION

In this section of the study, numerical simulations of the synchronization of the four-dimensional hyperchaotic system using the active control method will be conducted. The simulations were performed using MATLAB 2021a. During the simulation, the controller values $[k_1\ k_2\ k_3\ k_4] = [20\ 20\ 20\ 20]$ were chosen, with the parameters a and b set to 20 and 40/39, respectively. The initial conditions for the master hyperchaotic system were set to [1 1 1 1], while the initial conditions for the slave hyperchaotic system were set to [5 5 5 5]. The time evolution of the states of identical hyperchaotic systems with different initial conditions is shown in Figure 10, and the variations of the error dynamics are illustrated in Figure 11.

Figures 10 and 11 show that the identical novel 4-dimensional hyperchaotic system with different initial conditions synchronizes within a short period once the controller is activated at $t = 10s$. During synchronization, the controller is inactive between 8-10 s and becomes active between 10-12 s. In other words, the controller is activated at $t = 10$ seconds. As seen in Figure 11, once the controller is active, the errors in the states reach zero within a very short time. Thus, it is demonstrated that synchronization of the proposed 4-dimensional hyperchaotic system using the active control method is successfully achieved.

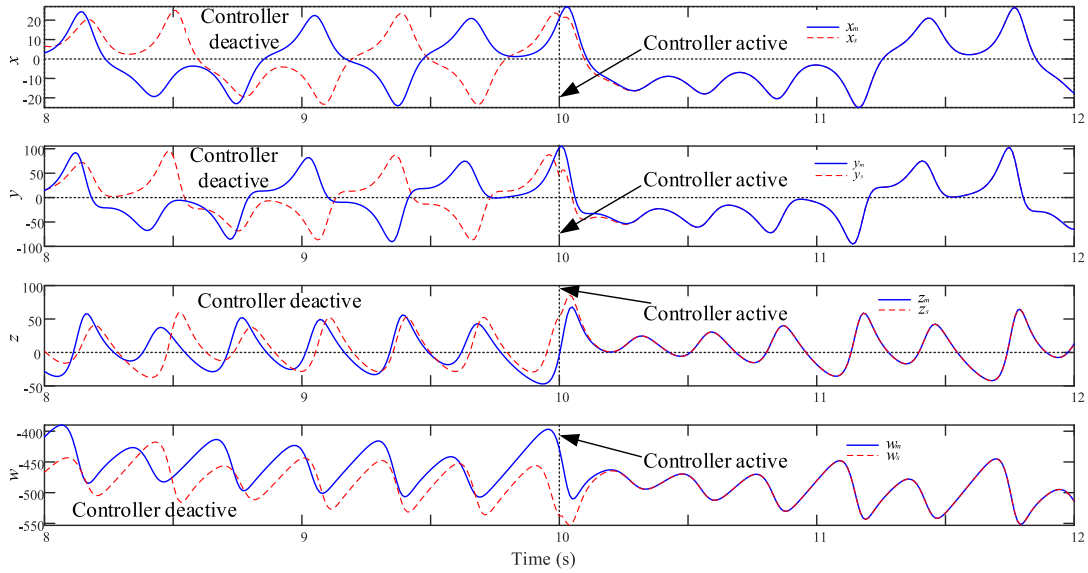

FIGURE 10. Time series of the states of the master and slave systems during synchronization.

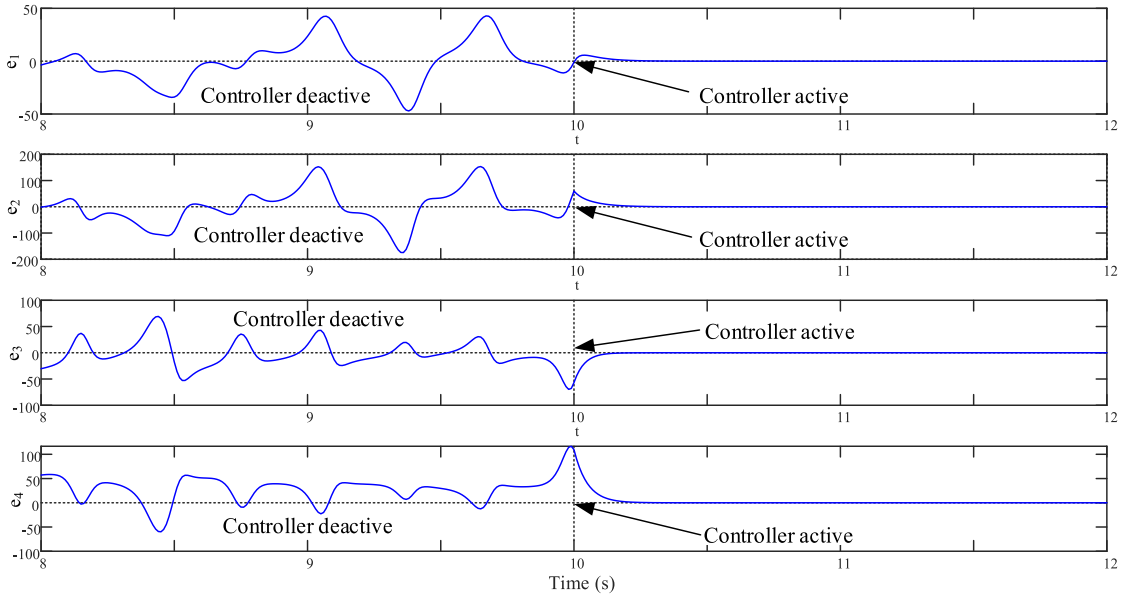

FIGURE 11. Time variation of the error during synchronization.

V. IMAGE ENCRYPTION AND DECRYPTION IMPLEMENTATION

In this section of the study, an image encryption application was implemented using the proposed hyperchaotic system. The encrypted image was then decrypted by the hyperchaotic system synchronized using the active control method. For the encryption image in the implementation phase, the 512 × 512 Elaine image, which is frequently used as a test image in image processing applications in the literature, has been used [36]. The implementation processes were carried out on a computer using MATLAB 2021a.

A. ENCRYPTION

The encryption process was generated by the master hyperchaotic system in the synchronization structure. During the encryption process, the values of the state variable x_m from the master hyperchaotic system were used to create a 512 × 512 encryption matrix, and the Elaine image was encrypted using the XOR operation. The 512 × 512 encryption matrix was created by sequentially taking $512 \cdot 512 = 262,144$ values from the state variable x_m after it reached a steady state. During the simulation, the initial conditions of the master hyperchaotic system were set to [1 1 1 1]. The diagram of the encryption structure is shown in Figure 12.

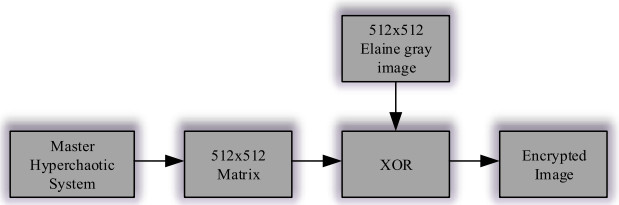

FIGURE 12. Block diagram of the encryption process.

The grayscale Elaine image used for encryption and the encrypted image obtained after encryption are shown in Figure 13.

FIGURE 13. (a) Original image, (b) Encrypted image.

As seen in Figure 13 (b), the encryption has been successfully performed.

B. ENCRYPTION PERFORMANCE

In this section, some methods used to demonstrate the success performance of the image encryption achieved using the proposed hyperchaotic system will be examined.

1) HISTOGRAM ANALYSIS

An obvious way to display an image's capacity to withstand attacks is with a histogram [37]. Because the original image's probability distribution of all pixel values is asymmetric, it is more vulnerable to assault. It is challenging to identify the patterns in the original image when using the suggested encryption approach because of the comparatively uniform and uneven probability distribution of the image's pixel values. The histogram analysis of the encrypted and unencrypted photos is displayed in Figure 14.

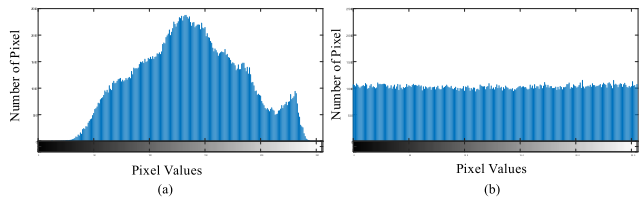

FIGURE 14. (a) Histogram of the original image, (b) Histogram of the encrypted image.

As can be seen from the histogram images in Figure 14, the histogram of the encrypted image is more uniform compared to the histogram of the unencrypted image, indicating that the encryption performed can withstand statistical attacks.

2) CORRELATION ANALYSIS

Following the encryption procedure, the degree of confusion in the image is reflected by the correlation analysis of neighboring pixels [38]. Figure 15 shows the horizontal, vertical, and diagonal correlation analysis images of the original and encrypted images.

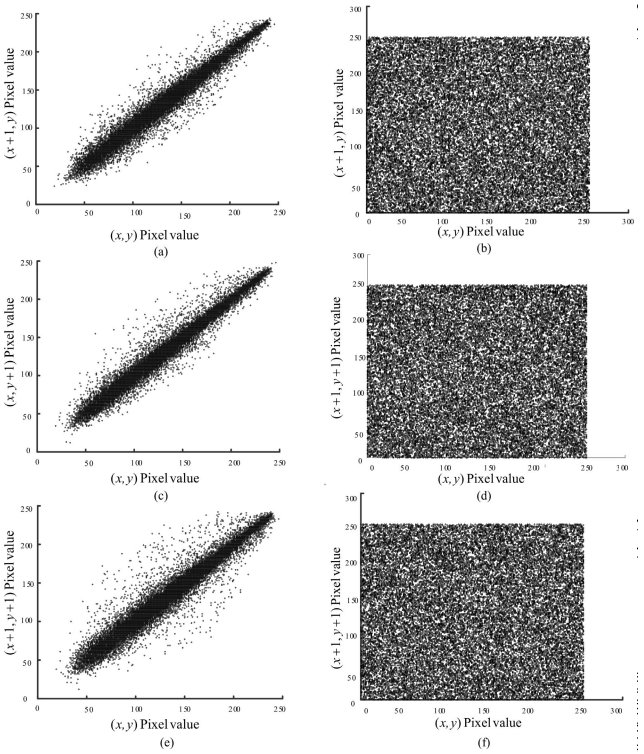

FIGURE 15. Correlation analysis graphs of adjacent pixels.

As illustrated in Figure 15, the unencrypted image exhibits a clear linear correlation. In contrast, the encrypted image displays a nearly random distribution of pixels in all directions, with almost no correlation across any direction. This indicates that while adjacent pixels in the original image are strongly correlated around a line, the pixels in the encrypted image are weakly correlated. This clearly demonstrates that the given encryption scheme can effectively withstand statistical attacks.

Furthermore, to calculate the correlation between pixels in the images, 10,000 samples were extracted from both the original and encrypted images. The correlation coefficients for horizontal, vertical, and diagonal directions were computed using the method described in (15).

$$
\begin{aligned}
E(x) &= \frac{1}{N}\sum_{i=1}^{N} x_i \\
D(x) &= \frac{1}{N}\sum_{i=1}^{N} (x_i - E(x))^2 \\
cov(x, y) &= \frac{1}{N}(x_i - E(x))(y_i - E(y)) \\
r_{x,y} &= \frac{cov(x, y)}{\sqrt{D(x)}\sqrt{D(y)}}
\end{aligned}
\tag{15}
$$

Here, r_{xy} represents the degree of confusion. The values obtained from the calculations for horizontal, vertical, and diagonal pixel values are presented in Table 3.

TABLE 3. Values of the circuit components used.

Pixel Direction	Original image	Encrypted image
Horizontal	0.9858	0.0219
Vertical	0.9844	0.0234
Diagonal	0.9748	0.0040

As observed from the correlation coefficient values obtained from adjacent pixels, the horizontal, vertical, and diagonal correlation coefficients for the original image are close to 1. These results indicate that the pixels in the original image exhibit high correlation. In contrast, the correlation coefficient values obtained for the encrypted image are close to 0, suggesting that there is negligible correlation between the encrypted image pixels. A graph depicting the correlation coefficients is shown in Figure 16.

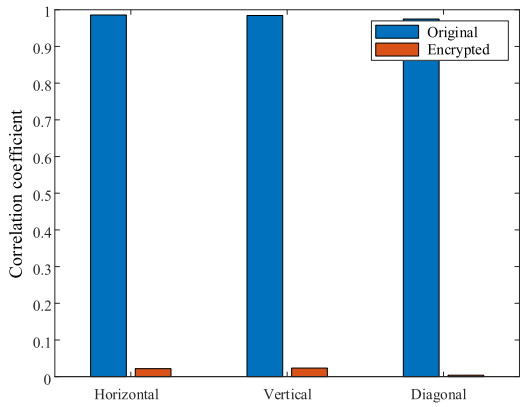

FIGURE 16. Graphical representation of correlation coefficients.

3) INFORMATION ENTROPY ANALYSIS

In image encryption implementations, the information entropy value of an image indicates the level of confusion and randomness among the pixels [39]. A high entropy value in an encrypted image signifies effective encryption. For grayscale images, a good encryption should result in an entropy value close to 8 [40]. The information entropy value is calculated using (16).

$$H(m) = -\sum_{i=0}^{255} p(m_i) \log_2 p(m_i) \tag{16}$$

The entropy value of the encrypted image was calculated to be 7.9911. This indicates that the encryption is considered effective in terms of information entropy.

4) DIFFERENTIAL ATTACK ANALYSIS

To reduce the risk of attacks, it is essential to minimize the similarity between the original image and the encrypted image. Two different methods are available to measure this similarity: The Number of Pixel Change Rate (NPCR) and the Unified Average Changing Intensity (UACI) [41]. An NPCR of 95% or higher indicates excellent diffusion. NPCR is calculated using (17), and UACI is calculated using (18).

$$NPCR = \frac{\sum_{i=1}^{M}\sum_{j=1}^{N} D(i,j)}{M \text{x} N} T\,100\% \tag{17}$$

$$UACI = \frac{1}{M \text{x} N} \text{x} \left[\sum_i \sum_j D_1(i,j) - \frac{D_2(i,j)}{256}\right] \times 100\% \tag{18}$$

The calculation results show that the NPCR value is 99.59% and the UACI value is 28.28%. The results are very close to the ideal values, indicating that the original image is highly sensitive. Upon reviewing the encryption performances, it is demonstrated that successful encryption has been achieved using the proposed hyperchaotic system.

C. DECRYPTION

In this section of the study, the encrypted image generated by the master hyperchaotic system will be decrypted to retrieve the original image. To obtain the original image, the slave hyperchaotic system, which was previously synchronized using active control, will be utilized. Similarly, to the method used to generate the 512×512 matrix for encryption, a 512×512 matrix is created here as well. During matrix generation, the values of the state variable x_s are used. In the simulation study, the initial values of the slave hyperchaotic system are taken as [5 5 5 5]. A block diagram of the decryption process is shown in Figure 17.

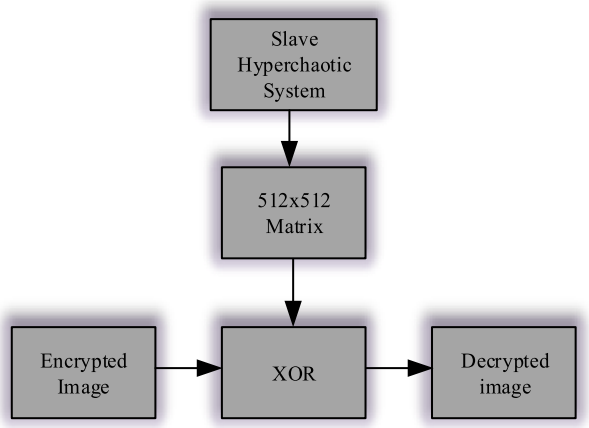

FIGURE 17. Block diagram of the decryption process.

The images obtained after encryption using the master hyperchaotic system and decryption using the slave hyperchaotic system are presented in Figure 18.

Figure 18 (b) and Figure 13 (a) clearly show that the original image was successfully recovered. The original Elaine image is obtained by the XOR of the encrypted Elaine image with the 512×512 matrix created using a slave hyperchaotic system with different initial values and used for decryption.

(a) (b)

FIGURE 18. (a) Encrypted image, (b) Recovered image.

Therefore, it can be concluded that the designed synchronization method works successfully.

VI. CONCLUSION

In this study, a novel four-dimensional hyperchaotic system, previously unused in the literature, is presented. To analyze the dynamic properties of the proposed system, Lyapunov exponents, bifurcation diagrams, phase portraits, Kaplan-Yorke dimension, and symmetry properties were examined in detail. The analyses confirmed that the system exhibits hyperchaotic behavior. Additionally, to test the physical feasibility of the system, circuit simulation was conducted using the Multisim 14.3 platform.

The synchronization of the proposed hyperchaotic system was designed using the active control method, and the performance of this design was evaluated through numerical simulations. By selecting appropriate control parameters in the synchronization design, the error induced when the controller was activated was reduced to zero in a very short time. This demonstrates that the design operates with high accuracy.

Encryption tests conducted in image encryption implementations revealed that the proposed hyperchaotic system performs successfully in encryption. Furthermore, decryption using the same synchronization structure was also successfully completed. The results indicate the physical feasibility of the proposed four-dimensional hyperchaotic system and confirm the effectiveness of the synchronization structure designed using the active control method in encryption and decryption implementations.

REFERENCES

[1] E. N. Lorenz, "Deterministic nonperiodic flow," *J. Atmos. Sci.*, vol. 20, no. 2, pp. 130–141, Mar. 1963.

[2] C. Sparrow, "6. The Lorenz equations," in *Chaos*. Princeton, NJ, USA: Princeton Univ. Press, 1986, pp. 111–134, doi: 10.1515/9781400858156.111.

[3] L. O. Chua, C. W. Wu, A. Huang, and G.-Q. Zhong, "A universal circuit for studying and generating chaos. I. Routes to chaos," *IEEE Trans. Circuits Syst. I, Fundam. Theory Appl.*, vol. 40, no. 10, pp. 732–744, Oct. 1993.

[4] G. Chen and T. Ueta, "Yet another chaotic attractor," *Int. J. Bifurcation Chaos*, vol. 9, no. 7, pp. 1465–1466, Jul. 1999, doi: 10.1142/s0218127499001024.

[5] J. Lü and G. Chen, "A new chaotic attractor coined," *Int. J. Bifurcation Chaos*, vol. 12, no. 3, pp. 659–661, Mar. 2002.

[6] J. Lü, G. Chen, D. Cheng, and S. Celikovsky, "Bridge the gap between the Lorenz system and the Chen system," *Int. J. Bifurcation Chaos*, vol. 12, no. 12, pp. 2917–2926, Dec. 2002, doi: 10.1142/s021812740200631x.

[7] O. E. Rössler, "An equation for continuous chaos," *Phys. Lett. A*, vol. 57, no. 5, pp. 397–398, Jul. 1976, doi: 10.1016/0375-9601(76)90101-8.

[8] J. Zhang, J. Hou, L. Xu, X. Zhu, and Q. Xie, "Dynamical analysis, circuit implementation, and simultaneous application of a novel four-dimensional hyperchaotic system based on cosine functions," *Microelectronic Eng.*, vols. 271–272, Mar. 2023, Art. no. 111939.

[9] F. Yu, W. Zhang, X. Xiao, W. Yao, S. Cai, J. Zhang, C. Wang, and Y. Li, "Dynamic analysis and FPGA implementation of a new, simple 5D memristive hyperchaotic Sprott-C system," *Mathematics*, vol. 11, no. 3, p. 701, Jan. 2023.

[10] X. Liu, X. Tong, M. Zhang, and Z. Wang, "A highly secure image encryption algorithm based on conservative hyperchaotic system and dynamic biogenetic gene algorithms," *Chaos, Solitons Fractals*, vol. 171, Jun. 2023, Art. no. 113450.

[11] S. Yan, L. Li, B. Gu, Y. Cui, J. Wang, and J. Song, "Design of hyperchaotic system based on multi-scroll and its encryption algorithm in color image," *Integration*, vol. 88, pp. 203–221, Jan. 2023.

[12] L. M. Pecora and T. L. Carroll, "Synchronization in chaotic systems," *Phys. Rev. Lett.*, vol. 64, no. 8, p. 821, 1990.

[13] S. K. Agrawal, M. Srivastava, and S. Das, "Synchronization of fractional order chaotic systems using active control method," *Chaos, Solitons Fractals*, vol. 45, no. 6, pp. 737–752, Jun. 2012.

[14] Y. Uyaroğlu and S. Emiroğlu, "Passivity-based chaos control and synchronization of the four dimensional Lorenz–Stenflo system via one input," *J. Vibrat. Control*, vol. 21, no. 8, pp. 1657–1664, Jun. 2015, doi: 10.1177/1077546313501186.

[15] K. Rajagopal, S. Vaidyanathan, A. Karthikeyan, and A. Srinivasan, "Complex novel 4D memristor hyperchaotic system and its synchronization using adaptive sliding mode control," *Alexandria Eng. J.*, vol. 57, no. 2, pp. 683–694, Jun. 2018.

[16] M. Roohi, M.-H. Khooban, Z. Esfahani, M. P. Aghababa, and T. Dragicevic, "A switching sliding mode control technique for chaos suppression of fractional-order complex systems," *Trans. Inst. Meas. Control*, vol. 41, no. 10, pp. 2932–2946, Jun. 2019, doi: 10.1177/0142331219834606.

[17] R. Gholipour, A. Khosravi, and H. Mojallali, "Multi-objective optimal backstepping controller design for chaos control in a rod-type plasma torch system using bees algorithm," *Appl. Math. Model.*, vol. 39, no. 15, pp. 4432–4444, Aug. 2015.

[18] S. Yan, E. Wang, Q. Wang, X. Sun, and Y. Ren, "Analysis, circuit implementation and synchronization control of a hyperchaotic system," *Phys. Scripta*, vol. 96, no. 12, Dec. 2021, Art. no. 125257.

[19] C. K. Volos, I. M. Kyprianidis, and I. N. Stouboulos, "Image encryption process based on chaotic synchronization phenomena," *Signal Process.*, vol. 93, no. 5, pp. 1328–1340, May 2013.

[20] S. Moon, J.-J. Baik, and J. M. Seo, "Chaos synchronization in generalized Lorenz systems and an application to image encryption," *Commun. Nonlinear Sci. Numer. Simul.*, vol. 96, May 2021, Art. no. 105708.

[21] Y. Xu, H. Wang, Y. Li, and B. Pei, "Image encryption based on synchronization of fractional chaotic systems," *Commun. Nonlinear Sci. Numer. Simul.*, vol. 19, no. 10, pp. 3735–3744, Oct. 2014.

[22] Y. Mao and G. Chen, "Chaos-based image encryption," in *Handbook of Geometric Computing*. Berlin, Germany: Springer-Verlag, 2005, pp. 231–265, doi: 10.1007/3-540-28247-5_8.

[23] W. Alexan, D. El-Damak, and M. Gabr, "Image encryption based on Fourier-DNA coding for hyperchaotic Chen system, chen-based binary quantization S-box, and variable-base modulo operation," *IEEE Access*, vol. 12, pp. 21092–21113, 2024. [Online]. Available: https://IEEExplore.IEEEorg/abstract/document/10422968/

[24] S. Emiroglu, A. Akgül, Y. Adiyaman, T. E. Gümüş, Y. Uyaroglu, and M. A. Yalçin, "A new hyperchaotic system from T chaotic system: Dynamical analysis, circuit implementation, control and synchronization," *Circuit World*, vol. 48, no. 2, pp. 265–277, Mar. 2022.

[25] T. Nestor, A. Belazi, B. Abd-El-Atty, M. N. Aslam, C. Volos, N. J. De Dieu, and A. A. Abd El-Latif, "A new 4D hyperchaotic system with dynamics analysis, synchronization, and application to image encryption," *Symmetry*, vol. 14, no. 2, p. 424, Feb. 2022.

[26] P. Li, J. Du, S. Li, and Y. Zheng, "Modulus synchronization of a novel hyperchaotic real system and its corresponding complex system," *IEEE Access*, vol. 7, pp. 109577–109584, 2019.

[27] S. Yan, B. Gu, E. Wang, and Y. Ren, "Finite-time synchronization of multi-scroll hyperchaotic system and its application in image encryption," *Math. Comput. Simul.*, vol. 206, pp. 391–409, Apr. 2023.

[28] J. He, W. Qiu, and J. Cai, "Synchronization of hyperchaotic systems based on intermittent control and its application in secure communication," *J. Adv. Comput. Intell. Intell. Informat.*, vol. 27, no. 2, pp. 292–303, Mar. 2023.
[29] A. Wolf, J. B. Swift, H. L. Swinney, and J. A. Vastano, "Determining Lyapunov exponents from a time series," *Phys. D, Nonlinear Phenomena*, vol. 16, no. 3, pp. 285–317, Jul. 1985, doi: 10.1016/0167-2789(85)90011-9.
[30] P. Frederickson, J. L. Kaplan, E. D. Yorke, and J. A. Yorke, "The Liapunov dimension of strange attractors," *J. Differ. Equ.*, vol. 49, no. 2, pp. 185–207, Aug. 1983.
[31] E. Ozpolat and A. Gulten, "Synchronization and application of a novel hyperchaotic system based on adaptive observers," *Appl. Sci.*, vol. 14, no. 3, p. 1311, Feb. 2024.
[32] B. K. Shivamoggi, "Chaos in dissipative systems," in *Nonlinear Dynamics and Chaotic Phenomena: An Introduction* (Fluid Mechanics and Its Applications), vol. 103. Dordrecht, The Netherlands: Springer, 2014, pp. 189–244, doi: 10.1007/978-94-007-7094-2_6.
[33] Y. Tong, Z. Cao, H. Yang, C. Li, and W. Yu, "Design of a five-dimensional fractional-order chaotic system and its sliding mode control," *Indian J. Phys.*, vol. 96, no. 3, pp. 855–867, Mar. 2022.
[34] K. Rajagopal, Y. Shekofteh, F. Nazarimehr, C. Li, and S. Jafari, "A new chaotic multi-stable hyperjerk system with various types of attractors," *Indian J. Phys.*, vol. 96, no. 5, pp. 1501–1507, Apr. 2022.
[35] E.-W. Bai and K. E. Lonngren, "Sequential synchronization of two Lorenz systems using active control," *Chaos, Solitons Fractals*, vol. 11, no. 7, pp. 1041–1044, Jun. 2000.
[36] B. Liu, X. Ye, and Q. Chen, "Generating infinitely many coexisting attractors via a new 3D cosine system and its application in image encryption," *IEEE Access*, vol. 9, pp. 136292–136301, 2021.
[37] A. Cohen, N. Nissim, and Y. Elovici, "MalJPEG: Machine learning based solution for the detection of malicious JPEG images," *IEEE Access*, vol. 8, pp. 19997–20011, 2020.
[38] P. N. Andono and D. R. I. M. Setiadi, "Improved pixel and bit confusion-diffusion based on mixed chaos and hash operation for image encryption," *IEEE Access*, vol. 10, pp. 115143–115156, 2022.
[39] E. Yavuz, R. Yazici, M. C. Kasapbasi, and E. Yamaç, "A chaos-based image encryption algorithm with simple logical functions," *Comput. Electr. Eng.*, vol. 54, pp. 471–483, Aug. 2016.
[40] K. U. Shahna and A Mohamed, "A novel image encryption scheme using both pixel level and bit level permutation with chaotic map," *Appl. Soft Comput.*, vol. 90, May 2020, Art. no. 106162.
[41] Y. Wu, J. P. Noonan, and S. Agaian, "NPCR and UACI randomness tests for image encryption," *Cyber J. Multidiscip. J. Sci. Technol. J. Sel. Areas Telecommun. (JSAT)*, vol. 1, no. 2, pp. 31–38, 2011.

ERMAN OZPOLAT was born in Elâzığ, Türkiye. He received the Ph.D. degree in electrical and electronics engineering from Firat University, Elâzığ, in 2024. He is currently a Doctoral Research Assistant with the Department of Electrical and Electronics Engineering, Muş Alparslan University. His research interests include chaos theory and chaos control and applications.

VEDAT CELIK was born in Elâzığ, Türkiye, in 1976. He received the B.S., M.S., and Ph.D. degrees from the Electrical and Electronics Engineering Department, Firat University, Elâzığ, in 1997, 2004, and 2010, respectively. He has been an Associated Professor with Firat University, since 2017. His current research interests include modeling and stability analysis of time delay systems, nonlinear dynamics and chaos, fractional order control and systems, and chaos synchronization.

ARIF GULTEN was born in Elâzığ, Türkiye, in 1970. He received the B.S. degree from Gazi University, Ankara, in 1993, and the M.S. and Ph.D. degrees from the Electrical and Electronics Engineering Department, Firat University, Elâzığ, in 1996 and 2003, respectively. He has been a Professor with Firat University, since 2019. His current research interests include chaos, chaos control, deep learning, and chaos synchronization.